8 Electronic Correlations and Metal-Insulator Transitions

Józef Spałek and Danuta Goc-Jagło

Institute of Theoretical Physics, Jagiellonian University,
ul. Łojasiewicza 11, PL-30-348 Kraków

8.1. Introduction: The Meaning of Localization – Delocalization Transitions in Solids with Examples

The concept of localization-delocalization transition is at the forefront of condensed matter physics as it is directly connected to delocalization of localized (atomic-like) states and a formation of a quantum liquid of itinerant (band) electrons. In the latter state, we talk often about an almost localized Fermi liquid. The situation is represented schematically in Fig. 8.1, where a lattice of hydrogenic-like states transforms into electron liquid, in which the skeleton of created thus ions (cations) remains intact. Obviously, the persistence of the atomic states of electrons in a solid is also nontrivial; one can intuitively expect that it is possible only under special circumstances, e.g., when the interatomic distance is large enough, so that particles located on the nearest neighboring atoms are in the states with their wave functions overlapping weakly. A quantification of all this is one of the subjects of this chapter. First we start with examples.

8.1.2. Crystallization of Liquid ^{3}He as Mott-Hubbard Transition

In the clearest form, this localization-delocalization transition is observed in three particular situations. First of them is the solidification of liquid ^{3}He, where the whole atoms can be regarded as quantum particles with (nuclear) spin 1/2 which below the boiling point $T_c \simeq 4.2$ K form the Fermi liquid [1]. Above the critical pressure (depending on temperature) this liquid crystallizes into a close-packed lattice. The phase diagram of condensed ^{3}He is shown in Fig 8.2. Note that in this case, contrary to the situation depicted

in Fig. 8.1, the freezing of He atoms comprises a spontaneous breakdown of the translational symmetry at the liquid-solid transition. The spontaneous freezing of quantum particle gas into lattice is independent of the quantum statistics of the particles (see below). Nonetheless, providing the mechanism for the localization and discussing the role of mutual interparticle interaction, at least in a model situation, is our principal task.

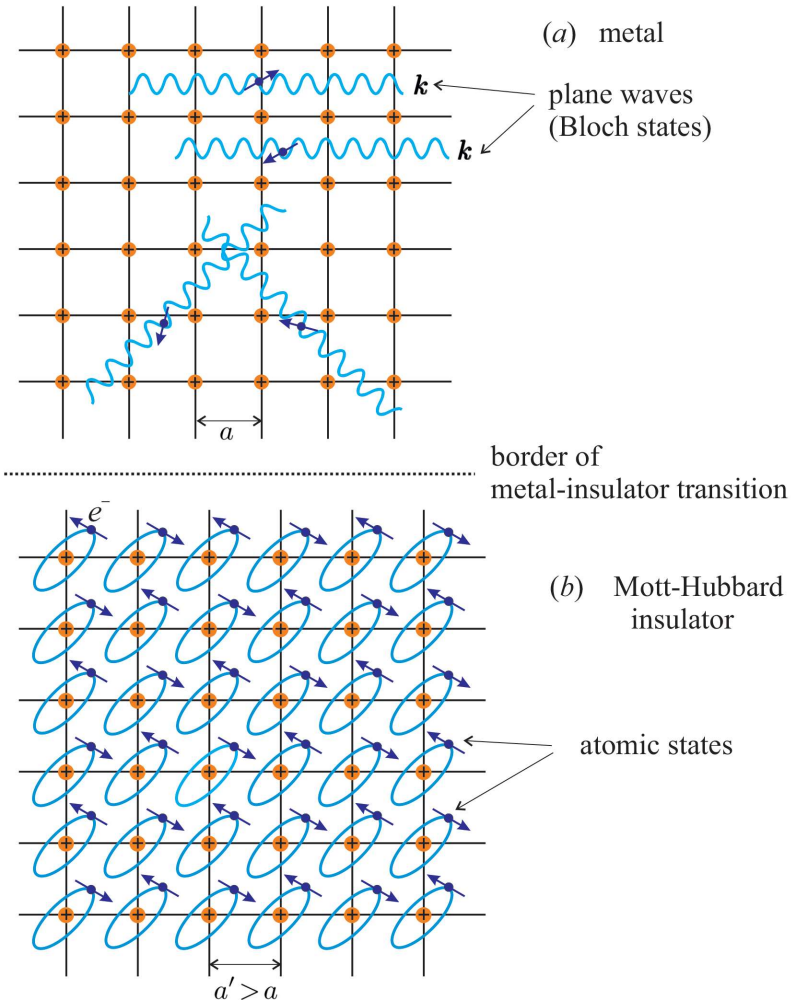

Figure 8.1. Illustrative representation of the metallic (a) and Mott insulating (b) (localized) states. Note that in the state (a) the electrons derive from the parent atoms (only positive cations K^+ are left) and form still a lattice, as even in the delocalized state electrons regarded as the only relevant quantum particles.

8.1.2. Localization-Delocalization Transition of Ultracold Atoms

The second example of localization-transition is provided by ultracold gases in optical lattice [2]. This example illustrates the role of the single-particle periodic lattice potential in the system of mutually interacting quantum particles. Namely, in distinction to electronic lattices, the shape (and the depth) of the trapping potential strength can be accurately changed even in the regime of the transition. Exemplary results are drawn in Fig. 8.3, where the superfluid states are also marked. Because of the possibility of changing easily the lattice spacing and the potential – well depth, the systems can be regarded as quantum simulators of many-body processes. Additionally, since the periodic potential is imposed by laser fields, the transition can be studied in this clearest form, i.e., without the accompanying effect of lattice distortion.

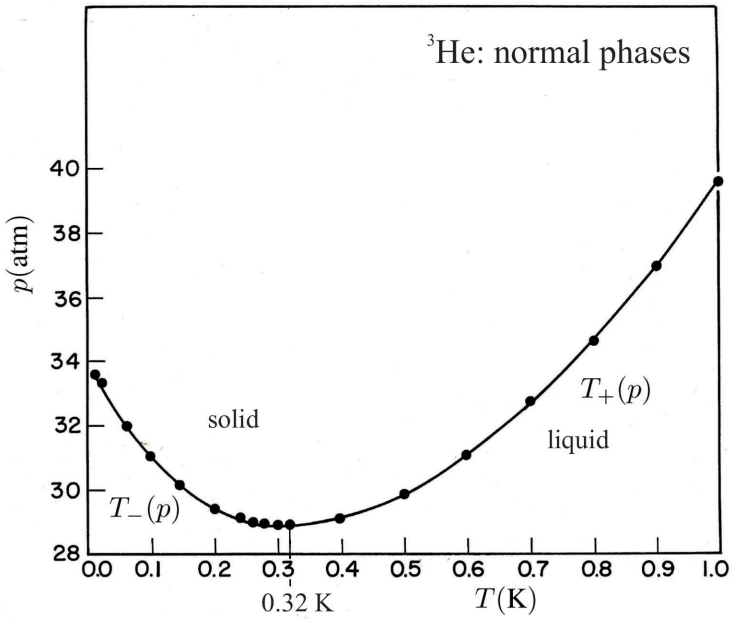

Figure 8.2. Schematic phase diagram on the pressure-temperature (p-T) plane involving only normal (non-magnetic, non-superfluid) phases. The meaning of the two curves $T_{\pm}(p)$ will be explained later in the text. The transition line is of the first-order character and a reentrant liquid phase is observed at low temperature $T < 0.32$ K. Note that the shape of the curve is attributed to the circumstance that the entropy of solid in large than that liquid. The same will appear for electron systems with metal-insulator transition as explained later. [cf. J. Spałek, Eur. Phys. J., **21**, 511 (2000)].

8.1.3. Metal-Insulator Transition in Doped V_2O_3

The third example is the canonical system – the chromium doped vanadium sesquioxide of the formula $(V_{1-x}Cr_x)_2O_3$, where x represents the portion of Cr atoms substituted for V. As V^{3+} ion contains two 3*d* electrons and Cr^{3+} has three, one would expect that we introduce into the system an extra 3*d* electrons so the system should be driven towards metallicity. In fact, the opposite is true as in the Cr^{3+} case 3*d* wave functions are tighter bound to its parent nucleus than those in the case of V^{3+}. Therefore, neglecting the disorder introduced by substitutions one may say that the bare bandwidth *W* of 3*d* states is reduced and upon a minute substitution Cr the pure V_2O_3 is driven towards the (Mott-Hubbard) insulating state, which means that then the system becomes an insulating Heisenberg antiferromagnet. Temperature dependence of electrical resistivity ρ vs. $1/T$ and the phase diagram of the doped system is shown in Fig. 8.4(a), (b) [3]. In Fig. 8.4(a) we observe discontinuous transitions: insulator-metal (from antiferromagnetic insulator (AFI) to paramagnetic metal (PM) one and from PM to paramagnetic insulator (PI)) follow by a gradual to (reentrant) transition back to the paramagnetic metallic (PM') phase. In the next Section, we

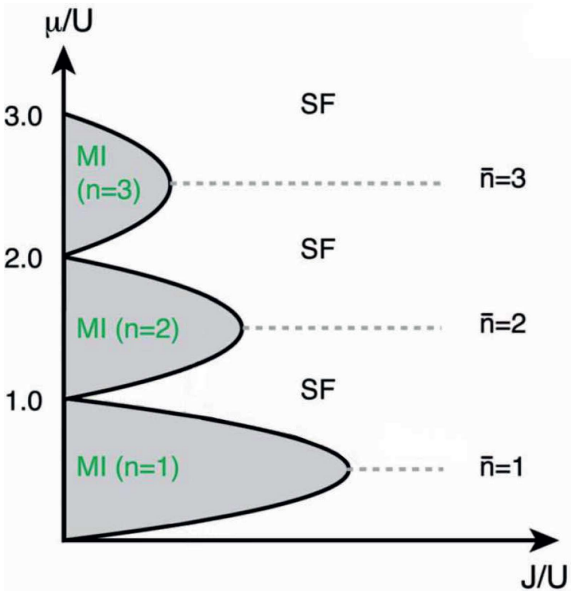

Figure 8.3. Schematic phase diagram for the bosons described by the Hubbard model. MI means Mott insulator, whereas SF – superfluid phase. This phase diagram is on the plane relative chemical potential – magnitude of the hopping to interaction (μ/U–t/U). Note that the Mott insulating (localized) phase can appear also for bosons. The phenomenon localization-delocalization transition is thus universal for a sufficiently large interaction amplitude *U* with respect to the amplitude of the particle hopping *J* between the neighboring sites (taken from [2]).

interpret these transitions within a simple scheme based on the Hubbard model as a starting point. Note that the changes of resistivity accompanying the transitions involve many-order jumps in resistivity, at temperatures in the range 120–350 K, so they must involve a rather radical alteration of the nature of relevant electronic states.

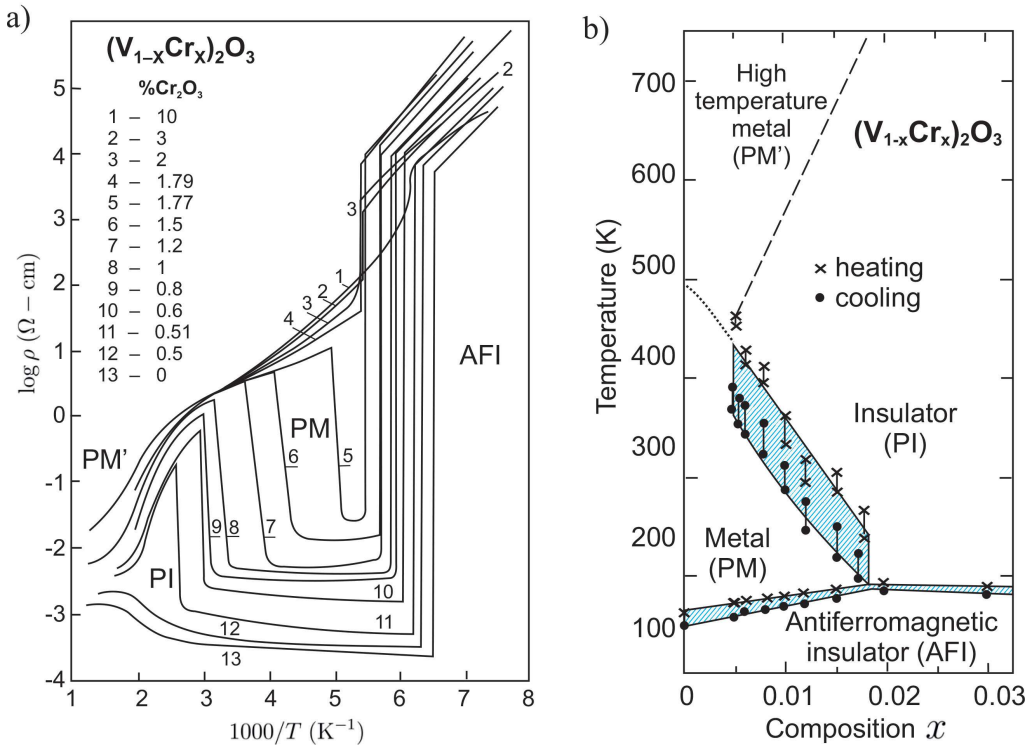

Figure 8.4. a) temperature dependence of the electrical resistivity (in logarithmic scale) vs. $1/T$ for Cr-doped V_2O_3. A very shape transition from antiferromagnetic insulating (AFI) to paramagnetic metallic (PM) phase is followed by a reverse PM → PI at higher temperature, which in turn is followed by PI → PM' crossover transition and a reentrant metallic (PM') transition at still higher temperatures. b) phase diagram for the same system on T-x plane; the hatched are depicts the hysteretic behavior accompanying the discontinuous transitions (taken from Ref. [3]), with small modifications.

A separate field of study is the effect of atomic disorder on the behavior of those correlated systems. Also, the role of interparticle interaction on the localization in nanophysical systems is particularly timely with the advent of nanotechnology. These are very important subjects and will be discussed briefly at the end.

8.2. Elementary Approach to the Metal-Insulator (Mott-Hubbard) Transitions

8.2.1. Normal metal as a Landau Fermi liquid: basic characteristics

The concept of ideal gas of electrons (in general, fermions) of spin $S = 1/2$ is well established. It is characterized by the Pauli principle (or the antisymmetry of N – particle wave function with respect to the two-particle coordinates ($(\boldsymbol{r}_1\delta_1)$ and $(\boldsymbol{r}_2\delta_2)$ transposition), from which a number of its basic properties follow. Those properties are described by characteristics listed in Table 8.1 for normal and correlated metals regarded as *Landau Fermi liquids.*

Table 8.1: Scaling laws of single-particle excitations in principal quantities of an almost localized Fermi liquid. The quantities are: $T^* = T/q$, $H^* = H_a/q$, $\beta^* = \beta/q$ and those with the subscript zero represent noninteracting particles, H_a is applied magnetic field, and β is the effective exchange field.

Property	Formula for noninteracting particles	Scaling property for ALFL
Leaner specific heat	$C_V = \gamma_0 T$	$\gamma = \gamma_0/q$
Pauli paramagnetism	$M = \chi_0 H_a$	$\chi = \chi_0(T^*)/qS$
Fermi temperature	$T_{F0} = \mu_0/k_B$	$T_F = T_{F0}/q$
Density of states	$\rho(\varepsilon) = \frac{1}{N}\Sigma_{\boldsymbol{k}}\delta(\varepsilon - \varepsilon_{\boldsymbol{k}})$	$\rho(E) = (1/q)\rho_0(\varepsilon)$
Free energy functional	$F_0 = E_0 - TS_0$	$F(T, H_a) = q[F_0(T^*, H^*, \beta^*) + \beta^* m] + Ud^2$
Particle-particle scattering time	$\tau(\varepsilon, T) = h/[(\varepsilon-\mu)^2 + (k_B T)^2]$	$\tau(\varepsilon, T) = \tau_0(q, T^*)$
Quasiparticle energy	$\varepsilon - \sigma H_a$	$E = q[\varepsilon - \sigma(H^* - \beta^*)]$
Wilson ratio	$R_W = \chi_0/\gamma_0$	$R_W = R_0/\tilde{S}, \quad 1 < R_W < 4$

To obtain the characteristics listed in Table 1 one describes the single-particle states by the (quasi)momentum $\boldsymbol{p} = \hbar\boldsymbol{k}$, where $\boldsymbol{k}$ is the wave vector of the corresponding matter wave of length $\lambda = 2\pi/|\boldsymbol{k}| \equiv 2\pi/k$. In the simplest situation, the Fermi liquid is characterized by individual energy $\varepsilon_{\boldsymbol{k}} = \hbar^2\boldsymbol{k}^2/2m^*$, where m^* is the renormalized-by-interactions effective mass. The states $|\boldsymbol{k}\sigma)$ are occupied up to the Fermi energy, which in this case is

$$\varepsilon_F = \frac{\hbar^2 \boldsymbol{k}_F^2}{2m^*} \equiv k_B T_F, \quad \text{with} \quad k_F = \left(3\pi^2 \frac{N}{V}\right)^{1/3}, \tag{8.1}$$

where T_F is the so-called Fermi temperature and k_F the corresponding wave vector. n In more general situation the electronic spectrum near the Fermi energy can be linearized, i.e., expressed as

$$\varepsilon_{\boldsymbol{k}} - \varepsilon_F \simeq \left.\frac{\partial \varepsilon_{\boldsymbol{k}}}{\partial \boldsymbol{k}}\right|_{kF} \cdot \left(\boldsymbol{k} - \boldsymbol{k}_F\right) = \hbar v_F \left(k - k_F\right), \tag{8.2}$$

where the expression after the second equality sign is valid for an isotropic in k-space electronic liquid and v_F is the Fermi velocity, which can be expressed also by $v_F = p_F/m^* = \hbar k_F/m^*$. In the case of multiple bands (characterized by the dispersion relations $\varepsilon_{\boldsymbol{k}} = \varepsilon_{\boldsymbol{k}n}$) we have multiple Fermi velocities $v_{Fn} = \hbar k_{Fn}/m_n^*$.

The next basic quantity is the density of states at the Fermi level. i.e.,

$$\rho\left(\varepsilon_F\right) = \frac{V}{\pi^2}\frac{m*}{\hbar^2}\left(3\pi^2\frac{N}{V}\right)^{2/3} = \frac{3}{2}N\varepsilon_F^{-1}, \tag{8.3}$$

for the case of electron gas; V is the system volume. Usually, the density is listed per particle per one spin direction; then (2.3) must be divided by $2N$. Note that if N is large ($\sim 10^{23}$), the number of available single-particle states in 1eV interval around the Fermi surface is enormous, so the energy distribution is a continuous function for all practical purposes.

For the sake of completeness, one has to add the distribution of particle energies at temperature T. For $T > 0$ it redistributes then around $\varepsilon_{\boldsymbol{F}} = \mu$ in accordance with the Fermi-Dirac distribution.

$$f\left(\varepsilon_{\boldsymbol{k}}\right) = \overline{n}_{\boldsymbol{k}\sigma} = \frac{1}{\exp\left[\beta\left(\varepsilon_{\boldsymbol{k}} - \mu\right)\right] + 1}, \tag{8.4}$$

where the energies $\{\varepsilon_{\boldsymbol{k}}\}$ are here spin-independent and μ is the chemical potential determined from the fact that the total number of particles in the system is established and equal to N_e, i.e.,

$$N_e = \sum_{\boldsymbol{k}\sigma}\overline{n}_{\boldsymbol{k}\sigma} = 2\sum_{\boldsymbol{k}}\frac{1}{\exp\left[\beta\left(\varepsilon_{\boldsymbol{k}} - \mu\right)\right] + 1}. \tag{8.5}$$

The summation for the system of N states runs over the first Brillouin zone (BZ) and $\beta = (k_B T)^{-1}$ is the inverse temperature in energy units (k_B is the Boltzmann constant). Note that $\mu = \mu(T, n)$, where $n = N_e/N$ is the so-called band filling. Also, $\mu(T = 0, n) = \varepsilon_F$. Other characteristics are discussed later.

8.2.2. Mott-Wigner Criterion of Localization

The Landau theory of Fermi liquids encompasses both the renormalized by-interaction basic characteristics, as well as the collective excitations – the sounds, all of which were treated first on a phenomenological basis. A full description also requires an elaboration of plasmon excitations for a charged liquid, with the corresponding damping of the modes [4]. Nonetheless, the theory does not address the situation when the interaction becomes comparable to the kinetic (band) energy of individual quasiparticles or even becomes predominant. The last two situations correspond to the case with the correlated or strongly correlated electrons, respectively.

To estimate the stability of the electron gas against localization induced by the interparticle interaction we start from expression for the average kinetic energy per particle which is

$$\bar{\varepsilon} = \frac{3}{5}\frac{\hbar^2}{2m^*}\left(3\pi^2\frac{N_e}{V}\right)^{2/3}. \tag{8.6}$$

If we define the particle density as $\rho \equiv N_e/V$, we see that in three-dimensional gas this energy increases with density as $\sim\rho^{2/3}$ (in d-dimensions it is $\sim\rho^{2/d}$). On the other hand, the average Coulomb interaction per particle can be estimated as

$$\varepsilon_{e-e} = \frac{e^2}{2\varepsilon r_s} = \frac{e^2}{2\varepsilon}\left(\frac{N_e}{V}\right)^{1/3} = \frac{e^2}{2\varepsilon}\rho^{1/3}, \tag{8.7}$$

where ε is the static dielectric constant of the system and $(V/N_e)^{1/3}$ is the average distance between the electrons. One sees that for $d = 3$ the interaction energy is $\sim\rho^{1/3}$ and hence the kinetic energy increases faster when ρ is larger than the critical value $\rho = \rho_c$. To determine this value we set $\bar{\varepsilon} = \varepsilon_{e-e}$. An elementary inspection into this identity leads us to the the following condition

$$a_B\rho_c^{1/3} \cong 0.2, \tag{8.8}$$

where $a_B \equiv \hbar^2\varepsilon/(me^2)$ is the effective Bohr radius for electron in an insulating medium with a well defined static dielectric constant ε and ρ_c is this critical density. This condition is called as the *Mott* (*or Mott-Wigner*) criterion for the localization threshold for particles in the gas. Note also that since $\rho_c \equiv r_c^{-1}$, the effective distance between the particles frozen on the lattice is then of the order of $5a_B$.

Interpretation of this reasoning is as follows. For $\rho < \rho_c$ the interaction energy $\varepsilon_{e-e} > \bar{\varepsilon}$, whereas for high densities ($\rho > \rho_c$) the kinetic energy dom-

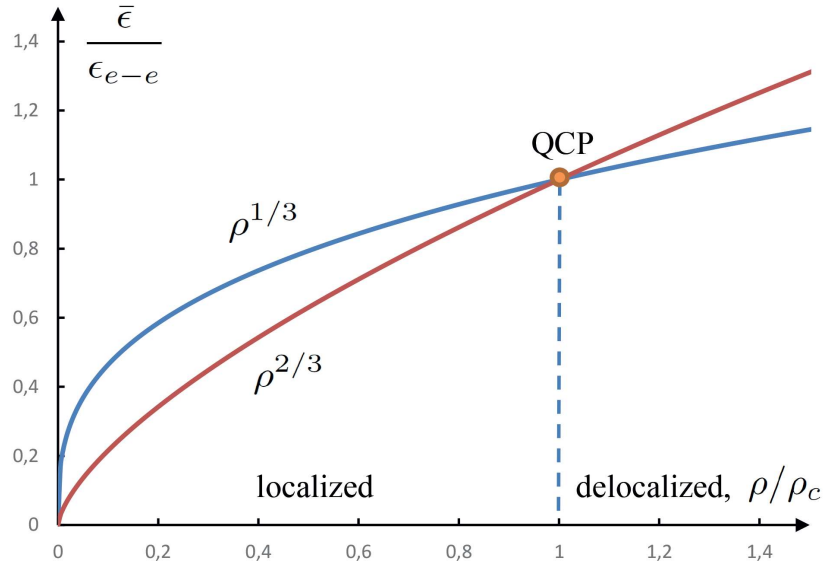

Figure 8.5. Schematic illustration of the transition between the delocalized (plane-wave) states of ideal electron gas and the localized (atomic, frozen) configurations of the Mott-Wigner type. This transition requires further analysis and is carried out next. The discussion relies on emphasizing a mutual competition between kinetic energy and repulsive interparticle Coulomb interaction.

inates. At the extreme densities $\rho \gg \rho_c$, $(\varepsilon_{e-e}/\bar{\varepsilon}) \to 0$ and hence the interacting gas approaches the limit of the ideal (non-interacting) gas even though $\varepsilon_{e-e} \to \infty$. A closer inspection leads us also to the conclusion that for $\rho < \rho_c$ the states are localized, since the dominating then repulsive interaction forces the particles to spread from each other as far away as possible (to the distance $\sim r_c$). Parenthetically, this is also the reason why the effective Bohr radius appears out of nowhere at this "critical point" ρ_c, even though there is no sign of any attractive atomic centers on which the electrons can establish atomic states. The mutual energetics is illustrated in Fig. 8.5. QCP denotes a quantum critical point if such a transition can be regarded as a continuous phase transition.

The purpose of this elementary reasoning is to show that the competing energies can lead to a qualitative change of character of physical states. Next, we will show on a slightly modified model – the Hubbard model – this peculiar type of physical behavior can indeed lead to true phase transitions in the $T \to 0$ limit for realistic (lattice) systems, starting with well define atomic states at large interatomic distances. Such a refined analysis is required since also the effective-mass value depends on the repulsive interaction magnitude. Also, we would like to model the situation with

electrons propagating in the periodic lattice of positively charged ions, not in a homogeneous positive and passive background charge, as is in our simple model. This last assumption is implicitly assumed in the above reasoning, since only then we can consider the electron gas as a stable system.

8.2.3 Localization on the Lattice: Hubbard Model

We start now with a lattice of atoms; for simplicity, we assume that each atom is contributing one electron to the system. Effectively, one can imagine a lattice of hydrogenic-like atoms with one valence electron each in the s-like state (cf. Fig. 8.1). Only the lattice of those initial s-like states will concern us and the question is when the assembly of electrons sits on atoms (in localized atomic states) and when, instead, they form a collective gas of interacting electrons confined by a remaining skeleton of positive ions, the latter playing only a passive role in the whole consideration. The question is what happens in between the two pictures?

The simplest Hamiltonian describing such an interacting gas on the lattice has been proposed by Hubbard (1963) and its explicit form is

$$\mathcal{H} = \sum_{\boldsymbol{k}} \varepsilon_{\boldsymbol{k}\sigma} n_{\boldsymbol{k}\sigma} + U \sum_{i} n_{i\uparrow} n_{i\downarrow}. \tag{8.9}$$

Here as before, $\varepsilon_{\boldsymbol{k}}$ is the energy of an individual particle in the spin nonpolarized state and with the wave vector $\boldsymbol{k}$, $n_{\boldsymbol{k}\sigma}$ is the number of particles in the single-particle state characterized by the quantum numbers ($\boldsymbol{k}$, σ), and $n_{i\sigma} = 0, 1$ is the number of electrons on given lattice site i with the spin σ. U is the interaction magnitude of contact (Hubbard) interaction when the two particles with opposite spins meet on the same atomic site i. At first look, this Hamiltonian has no connection to the reasoning of the preceding subsection, but not quite so. The rationale behind the similarity is following one. The energy $\varepsilon_{\boldsymbol{k}}$ varies in the interval $[-W/2, W/2]$ (we assume that the reference atomic energy of each particle can be regarded as $\varepsilon_{at} = 0$). The quantity W is called the bandwidth and the single-particle part (the first term) is more negative (the energy is smaller) if W increases. If we assume that the energies are spread uniformly, the average energy per particle is $-W/4$. The average interaction energy per pair of particles is $U\langle n_{i\uparrow} n_{i\downarrow}\rangle$. If we have one particle per atom, then the mean-field (Hartree-Fock) estimate is $\langle n_{i\uparrow} n_{i\downarrow}\rangle \simeq \langle n_{i\uparrow}\rangle\langle n_{i\downarrow}\rangle = 1/4$. In effect, the two energies balance out each other when they are of the same magnitude, i.e., when

$$E \equiv \langle \mathcal{H} \rangle = -\frac{W}{4} + \frac{U}{4} = 0, \tag{8.10}$$

i.e., when $U = W$. This condition replaces now the former condition (8.8) and physically amounts to the same. Namely, if $W > U$ then the single-particle ("kinetic") energy dominates and the fluid with $\{\boldsymbol{k}\}$ as a good quantum number is realized. The new principle is that in the opposite limit, the double occupancies, characterized by joint probability $\langle n_{i\uparrow} n_{i\downarrow}\rangle$, vanish. But all this requires a more careful study as the last statements represent assumptions of a more detailed quantitative approach. Such an analysis is provided next.

8.2.4. Quantitative Discussion of the Metal-Insulator Transition

The basic quantitative question we face when discussing the localization-delocalization transition is as follows. The kinetic (now band) energy of electrons in the delocalized state is of the order $W \sim 1$–3 eV per particle. We are interested in considering the limit $U \gtrsim W$. The thermal energy in the interesting us range is $k_B T \cong 10$ meV ≈ 100 K. The principal question is then how is it possible that such a small external thermal stimulus can drastically change the character of electronic states from itinerant to localized states or vice versa? Note also that this is a macrostate containing $\sim 10^{23}$ particles. The shortest answer we can provide is that close to the transition the energies in (8.10) almost compensate each other, making thus the system extremely sensitive to small perturbations such as the thermal stimulus, external pressure or chemical doping. Parenthetically, it is worth noting that the metallic state is a robust state of matter. A separate class is the state with localized electrons, regarded also as another such a universal state. The question is: when they become unstable, one with respect to the other?

To put this argument on a more quantitative basis we assume that the correlation function $\eta \equiv \langle n_{i\uparrow} n_{i\downarrow}\rangle$ is a new basic physical parameter, in addition to the individual particle energies $\{\varepsilon_{\boldsymbol{k}}\}$ and the interaction parameter U. The parameter η will differentiate between the delocalized and localized states in the following manner:

$$\eta = \begin{cases} \langle n_{i\uparrow}\rangle \langle n_{i\downarrow}\rangle = \frac{1}{4} & \text{for} \quad U = 0; \\ 0 \quad \text{for} \quad U \to \infty. \end{cases} \tag{8.11}$$

In other words, η plays in this very intuitive formulation the role of the order parameter, i.e., is the basic quantity which introduces the interelectronic (local) correlations. The task is to determine the explicit form of the dependence of the thermodynamic Landau-type functional on the parameter η.

At this point, we make a further assumption that since the two terms composing the total energy are of comparable magnitude, there appears

renormalization by the interaction of the kinetic energy part assumed in the following form

$$\varepsilon_{\boldsymbol{k}} \to \Phi\varepsilon_{\boldsymbol{k}} \equiv E_{\boldsymbol{k}}, \quad \text{with} \quad 0 \le \Phi \le 1, \tag{8.12}$$

where $\Phi \equiv \Phi(\eta)$ and has the following property

$$\Phi(\eta) = \begin{cases} 1 & \text{for} \quad \eta = \langle n_{i\uparrow}\rangle\langle n_{i\downarrow}\rangle = \frac{1}{4} \quad (\text{for} \quad U = 0) \\ 0 & \text{for} \quad \eta = 0 \quad (\text{for} \quad U \ge U_c). \end{cases} \tag{8.13}$$

These two conditions mean respectively, that the band energy takes the usual form ($E_{\boldsymbol{k}} = \varepsilon_{\boldsymbol{k}}$) when $U \ll W$ and that the band energy and the interaction energies disappear when $U \gg W$ ($\Phi\varepsilon_{\boldsymbol{k}} = U\eta = 0$). This last condition amounts to what we term as the perfect compensation of the two competing energies. It takes place, we expect, around $U \approx W$.

Explicitly, we have in view the situation when $U \to W$. Then, in the spirit of Landau expansion for the order parameter, we may assume that $\Phi(\eta) = f_0 + f_1\eta + f_2\eta^2 + o(\eta^3)$. The coefficients f_0, f_1, and f_2, which are assumed as independent of U/W, are determined from the known limiting situations (2.13), together with as the fact that $\eta = 1/4$ for $U = 0$. The sets of conditions, when implemented to the modified expression ($\langle\mathcal{H}\rangle$), lead

$$E \equiv \langle\mathcal{H}\rangle / N = \Phi(\eta)\bar{\varepsilon} + U\eta. \tag{8.14}$$

The explicit expression for η is obtained from the Landau-type minimization condition $\partial E/\partial\eta = 0$ for $\eta = 1/4$, leads to the explicit result for $\Phi(\eta)$, namely

$$\Phi(\eta) = 8\eta(1 - 2\eta). \tag{8.15}$$

Furthermore, the explicit results for all the involved quantities are then after minimization of E with respect to η equal to

$$\eta \equiv \eta_0 = (1/4)(1 - U/U_c), \tag{8.16}$$

$$\Phi \equiv \Phi_0 = \left[1 - \left(\frac{U}{U_c}\right)^2\right], \tag{8.17}$$

$$E_G = \bar{\varepsilon}\left(1 - \frac{U}{U_c}\right)^2, \tag{8.18}$$

where now $U_c \equiv 2W$ and $\bar{\varepsilon} = -W/4$. We thus see that all the quantities scale with U/U_c and hence, the value U_c plays the role of the uppermost critical value, up to which the metallic (delocalized) state of particles is stable. This critical value replaces the criterion (8.8) which valid for electron gas.

It is determined by the bare bandwidth W and thus, at least qualitatively, is independent of crystal structure under the proviso that we have a single band with correlated electrons, and all other bands are energetically separated from it. With this formulation we cannot go beyond the value $U = U_c$. Namely, for $U > U_c$ the state is that of atomic states on the lattice, i.e., that of *the Mott-Hubbard insulating state*. For all the practical purposes, the state is then that of a *Heisenberg antiferromagnet*, depicted schematically in Fig. 8.1. One should note that the system remains insulating even above the Néel temperature, as discussed in detail below. However, the inclusion of antiferromagnetic state requires an essential extension of the present approach to incorporate, among others, the exchange interactions in the insulating phase, which in turn is the starting point to the discussion of temperature low-T regime the metal-insulator transition, comprising also the magnetic states. We quote the results, not elaborated here[1], which document explicitly the critical behavior as $U \to U_c \equiv 8|\bar{\varepsilon}| = 2W$. Namely, the static magnetic susceptibility at $T = 0$ of the system in the delocalized state is

$$\chi = (\chi_P)/\Phi_0 \left[1 - \frac{U}{W} \frac{1 + U/(2U_c)}{(1 + U/U_c)^2} \right]^{-1}, \tag{8.19}$$

where χ_P is the Pauli susceptibility for the noninteracting electron gas. If $U \to U_c - 0$ then[2]

$$\chi \sim \frac{\chi_P}{\Phi_0} \to \infty \quad \text{for} \quad U \to U_c, \tag{8.20}$$

where the optimal value of $\Phi = \Phi_0$ is denoted by q in Table 8.1.

There is a clear sign of singularity when $\Phi \to 0$. Moreover, probably the most spectacular feature associated with this transition is the behavior of the magnitude of spin $\boldsymbol{S}_i$ when $U \to U_c$. It amounts to the relation [10, 11]

$$\left\langle \boldsymbol{S}_i^2 \right\rangle = \frac{3}{8}\left(1 + \frac{U}{U_c} \right) \to \frac{3}{4} \quad \text{for} \quad U \to U_c. \tag{8.21}$$

Note that as $U = U_c$ $\langle \boldsymbol{S}_i^2 \rangle \to$ reaches the value $3/4 \equiv 1/2(1/2+1)$, i.e., we recover the full atomic spin 1/2. The Mott insulator is thus indeed a quantum Heisenberg spin system. This sole result shows clearly, under

[1] For a detailed summary of the results obtained for such a mean-field picture see e.g.: J. Spałek, J. Sol. St. Chem. **88**, 77–93 (1990).

[2] Note also that there is also another singularity when the other factor [...] = 0. This corresponds to the so-called *Stoner instability* for the onset of ferromagnetism, which is not discussed here.

what conditions we can regard the systems as a lattice composed of (1/2) spins. We see that this is not at all a trivial assumption, since it requires a formation of stable atomic states on the lattice. Simply put, the electrons in atomic states in a solid appear then in the singly-occupied states, since the energy of their a motion (hopping) from site to site requires an increase of energy by U, the energy which exceeds by far the gain in kinetic energy ($-W/4$). *This is the reason for the existence of spins of atomic character in a solid, i.e., the state electronically entirely different from that of a metal, characterized by the band structure, renormalized masses of carriers the Fermi surface, and the absence of Pauli susceptibility.*

8.2.5. Quasiparticle Representation of Correlated-Electron System and the Phase Diagram

So far we have dealt with $T = 0$ transformation of itinerant to localized charge carriers or vice versa. The fact that measurable physical quantities are divergent at that point tells us that, at least within this simple scheme, the many-particle quantum states can become then singular. Obviously, one is not able to do measurements at $T = 0$ directly. Therefore, a natural question arises whether one can generalize these results to $T > 0$, which would reduce to those just discussed when the limit $T \to 0$ is taken in a straightforward manner. This is the task we are going to address next.

First, one should note that the single-particle part of energy in (8.14) is multiplied by $\Phi(\eta)$. Here we make a bold assumption that may seem natural to define renormalized individual single-particle states, i.e., assume that $E_k = \Phi\varepsilon_k$. The reason for this renormalization of each individual quantum single-particle state is that then we can write that at $T = 0$ we have

$$\Phi(\eta)\bar{\varepsilon} = \frac{1}{N}\Phi\sum_{k\sigma}\varepsilon_k n_{k\sigma} \equiv \frac{1}{N}\Phi\sum_{k<k_F\sigma}\varepsilon_k = \frac{1}{N}\sum_{k<k_F\sigma}(\Phi\varepsilon_k) = \sum_{k<k_F\sigma}E_k \quad (8.22)$$

Hence we may say that in this (correlated) quantum liquid the correlated character is acquired by the renormalized individual energies $E_k = \Phi\varepsilon_k$. We also assume that to the first approximation those quasiparticles of energy E_k obey still the Fermi-Dirac distribution[3] at $T > 0$, i.e.,

[3] This assumption is in the spirit of Landau (1956) theory of Fermi liquids; cf. J. Spałek, in *Reference Module in Materials Science and Materials Engineering* (Elsevier, Oxford, 2016) pp. 1–20. However, one must emphasize that the Landau theory of Fermi liquid does not comprise any discussion of particle localization into the Mott state localized spins.

$$n_{k\sigma} \equiv f_{k\sigma} = \frac{1}{exp\left[\beta\left(E_{k\sigma} - \mu\right)\right] + 1}, \tag{8.23}$$

where μ is the chemical potential. For interesting us case of one electron per atom one can take $\mu \equiv 0$, i.e., it is placed in the middle point of the band energies ranging from $-W/2$ to $W/2$, since we assume that the particle-hole symmetry holds, i.e., the energy is symmetric with respect to the middle point of the band. Note again that we have put the quasiparticle energies into the Fermi function, in the spirit of Landau the Fermi-liquid theory.

With those assumptions one can write down explicitly the Landau-type free-energy functional for the system of fermions in the following manner [10, 11].

$$\frac{\mathcal{F}}{N} = \frac{1}{N}\sum_{k\sigma} E_k f_{k\sigma} + U\eta + \frac{k_B T}{N}\sum_{k\sigma}\left[f_{k\sigma} \ln f_{k\sigma} + \left(1 - f_{k\sigma}\right) ln\left(1 - f_{k\sigma}\right)\right], \tag{8.24}$$

where now $\eta = \eta(T)$ plays, as above, the role of the temperature-dependent order parameter. The first two terms represent the effective internal energy, whereas the last is the entropy contribution in given configuration characterized by $\eta(T)$. The true free energy (equal to the Gibbs energy as $\mu \equiv 0$) is found from the minimum conditions:

$$\frac{\partial \mathcal{F}}{\partial \eta} = 0; \quad \frac{\partial^2 \mathcal{F}}{\partial \eta^2} > 0. \tag{8.25}$$

The value of $\eta \equiv \eta(T)$ obtained in this manner, when substituted to (8.24), determines the physical free energy $F \equiv F_{met}(T)$. One sees that the simplest (mean-field-type) theory is much more involved in the case of fermions (quantum particles) compared to that for pure spin systems, as it contains logarithmic contribution to the entropy, the part that cannot be expanded in the even powers of the order parameter directly.

The analysis of the solution of (8.24) is subtle and in general case, must be carried out numerically [5]. For the sake of simplicity, it is sufficient to limit to the low-temperature limit, which we overview briefly next. The results for Landau-function expression to the order at T^2 is

$$\frac{\mathcal{F}}{N} = -\Phi\frac{W}{4} + U\eta - \frac{\gamma_0 T^2}{2\Phi} + o\left(T^4\right). \tag{8.26}$$

The first two terms appeared before, the third represents the thermal excitations across the Fermi level located at $\mu \equiv 0$, and the quantity γ_0/Φ represents the renormalized linear-specific heat (Sommerfeld) coefficient, with

$$\gamma_0 = \frac{2\pi^2}{3} k_B^2 \rho(0), \tag{8.27}$$

being its unrenormalized and $\rho(0)$ is the density of unrenormalized states at the Fermi level (per atom per spin). Note that in our simplified discussion $\rho(0) = 1/W$. One additional warning is in place at this point. Namely, (8.26) becomes a singular expression for $\Phi \to 0$ and $T > 0$. Therefore, one sees that a singular jump to the $\eta = 0$ state is possible. Fortunately, it is the physics that comes to the rescue to avoid that and tackle it properly. Namely, as we have noted earlier, the fermionic liquid is assumed to transform to a system of localized moments. In the latter state, the free energy is also nonzero, and neglecting the exchange interaction among the spins (magnetic order ignored), it can be written in the form

$$\frac{F_{ins}}{N} = -k_B T \ln 2, \tag{8.28}$$

i.e., we include only the entropy part of freely fluctuating spins $S = 1/2$. In effect, if we are interested in a discontinuous (first-order) transition, the condition is that $F_{met} = F_{ins}$, where F_{met} is the physical free energy of the delocalized (metallic) state obtained after minimization of F with respect to η, combined with its low-T expansion. In what follows, we discuss only the final results [3, 4, 5].

Let us define $I \equiv U/U_c$. The functional (8.26) transforms then into an intuitively clear expression for the free energy, namely

$$\frac{F_{met}}{N} = (1-I)^2 \bar{\varepsilon} - \frac{\gamma_0 T^2}{1-I^2} + o\left(T^4\right). \tag{8.29}$$

Equating (8.28) and (8.29) we obtain two transition temperatures. Explicitly,

$$\frac{k_B T_{\pm}}{W} = \frac{3}{2\pi^2}\left[1-\left(\frac{U}{U_c}\right)^2\right]\left\{(\ln 2)^2 \pm \left[(\ln 2)^2 - \frac{1-U/U_c}{1+U/U_c}\right]^{1/2}\right\}. \tag{8.30}$$

This result is depicted in Fig. 8.6 (as before, $U_c = 2W$). The lower temperature branch (T_-) is drawn as a solid line, whereas the T_+ part is actually a crossover line, not accounted properly by making our low-T expansion. The T_- ends up in a classical critical point which determines the lowest value of $U = U_{lc}$, determined the condition from $T_+ = T_-$, below which the delocalized states are always stable. The value of the critical temperature T_c is

$$\frac{k_B T_c}{W} = 1 - \frac{3\ln 2}{2\pi^2}\left[1-\left(\frac{U_{lc}}{U}\right)^2\right]. \tag{8.31}$$

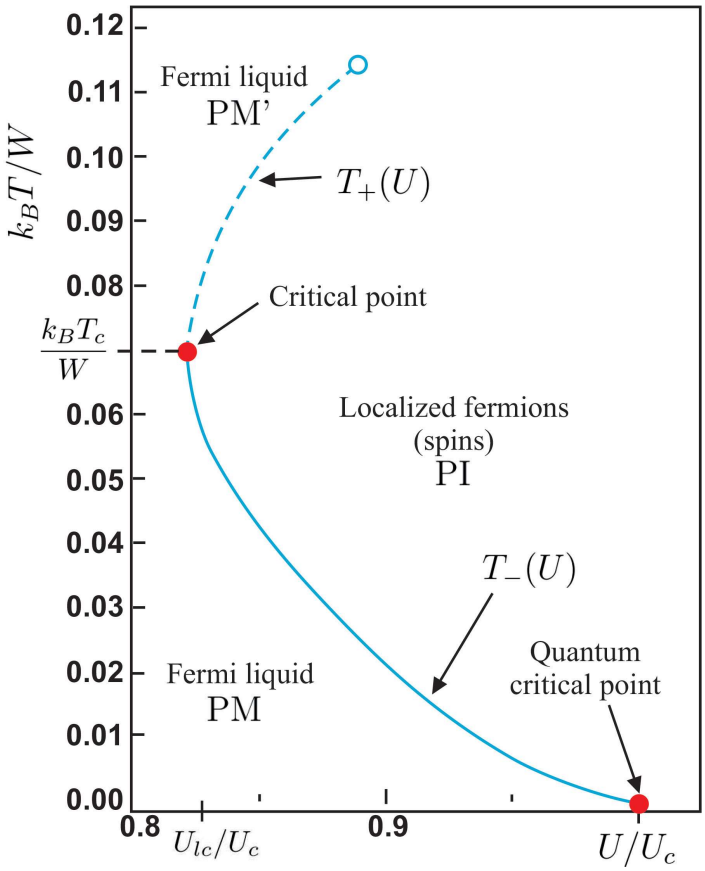

Figure 8.6. Phase diagram in the paramagnetic (PM, PI) regions of the metal-insulator transition. The critical points and characteristic temperatures are marked explicitly; the points (T_c, $T_c = 0$) terminate the first-order (blue solid) line.

The value of $T_c = 0$ appears for $U = U_c = 2W$. This critical point can be called a *quantum critical point* (QCP) as the entropy is zero and the two mechanical energies compensate each other. On the other hand, the solid line in between T_c and zero represents the line of discontinuous transitions, as is illustrated further in Fig. 8.7, where we have drawn the free energies of the two phases. The curves *a*–*e* depict the evolution from of Fermi liquid state the low $U < U_{lc}$ region, for the $U \to U_c$ limit. When the parabola is tangent to the straight line (between *a* and *b*) we reach the lower critical value U_{lc} for the transition to take place. Furthermore, for U between U_{lc} and U_c we observe two transitions. The point $U = U_c$ is singular as both curves coalesce into a single QCP. Moreover, for $U \in (U_{lc}, U_c)$ the two curves intersect at a non-zero angle, which means that then the entropy $S = -\partial F/\partial T$ jumps when the transition takes place. Hence, it is a first-order transition except the points $U = U_{lc}$ and U_c. Strictly speaking, the QCP

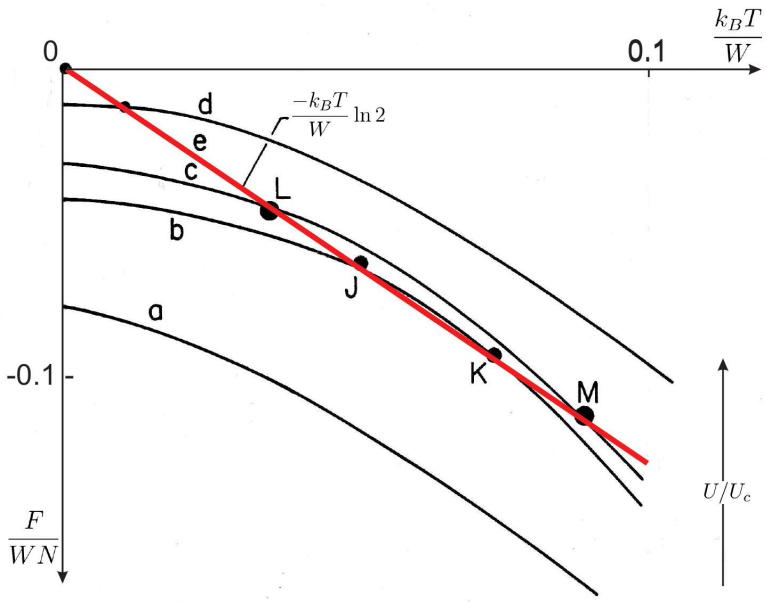

Figure 8.7. Plots of temperature dependence of free energy in the paramagnetic state: The parabolas $a - e$ represent the energy of the metallic (Fermi-liquid) state with ascending U/U_c ratio. The straight line (in red) represents the energy of the Mott insulating (PI) state. The points of crossing L and J correspond to a discontinuous PM → PI transition, whereas those at K and M correspond to the reverse PI → PM' transition. The transition to the high-T PM' metallic phase can also take the form of a crossover behavior. Note that the competitions between the energy and the entropy contribution in creating the two transition, both of the Mott type at $T > 0$.

becomes a *hidden critical point* when we include the exchange interaction in the localized phase, but this topic will not be touched upon here.

Finally, we would like to present the theoretical version of the phase diagram drawn in Fig. 8.4(b) results of our simple theoretical approach are displayed in Fig. 8.8, together with the experimental results of Fig. 8.4(b) in the inset. The symbol AFS means the *Slater (band) insulator*, with the so-called Slater splitting of the original band into two subbands and caused by the antiferromagnetic ordering. The principal difference between the AFS and AFI states is that the former becomes metallic (PM) above the Néel temperature, so we recover the delocalized states when the gap due to the antiferromagnetic superstructure disappears. The gap remains in the Mott (PI) phase even though the antiferromagnetic is absent. A systematic evolution of the Slater gap to its Mott-Hubbard correspondent as a function of the relative interaction strength has been analyzed elsewhere [5]. A similar evolution of the system (in the opposite direction) takes place also for $NiS_{2-x}Se_x$ [6] and other systems [7].

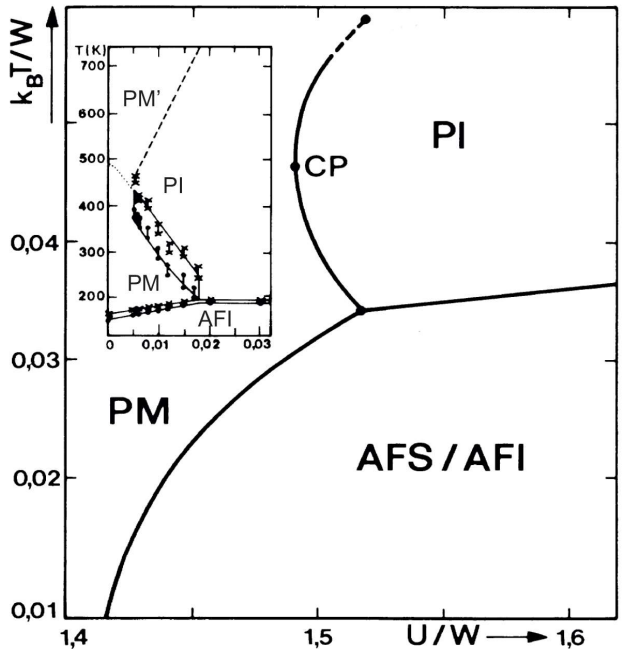

Figure 8.8. Phase diagram on the plane $T - U/W$ of possible metal-insulator transitions. Note reentrant metallic phases on sandwiching antiferromagnetic-Slater (AFS) and paramagnetic-insulating (PI) phase, and one at the high temperatures. Inset: Experimental transitions in the $T - x$ plane for $(V_{1-x}Cr_x)_2O_3$. For details see main text.

8.2.6. Mott-Hubbard Localization in Correlated Nanoscopic Systems

As we have seen already in Fig. 8.1, the Mott-Hubbard transition is in its essence a transition between atomic and itinerant (band) states in a solid or other quantum condensed-matter system. An interesting question is how this evolution will look in the case of a nanoscopic system? Related to that is the question of how small a piece of quantum wire can have preserved some of the principal metallic characteristics? These problems can be modeled in a simple manner by considering a linear chain of atoms with s-like valence electrons, one electron per atom. Additionally, both open chains as well as those with periodic boundary conditions can be considered. In Figs. 8.9–8.11 we present exemplary results. First, in Fig. 8.9 the statistical distribution function $n_{k\sigma}$ is drawn, for selected interatomic distances $R/a_0 = 2$–5, where a_0 is the 1s Bohr radius. We note three characteristic features. First, the exact results arrange themselves into the systematic pattern for different values of the number of atoms N. Second,

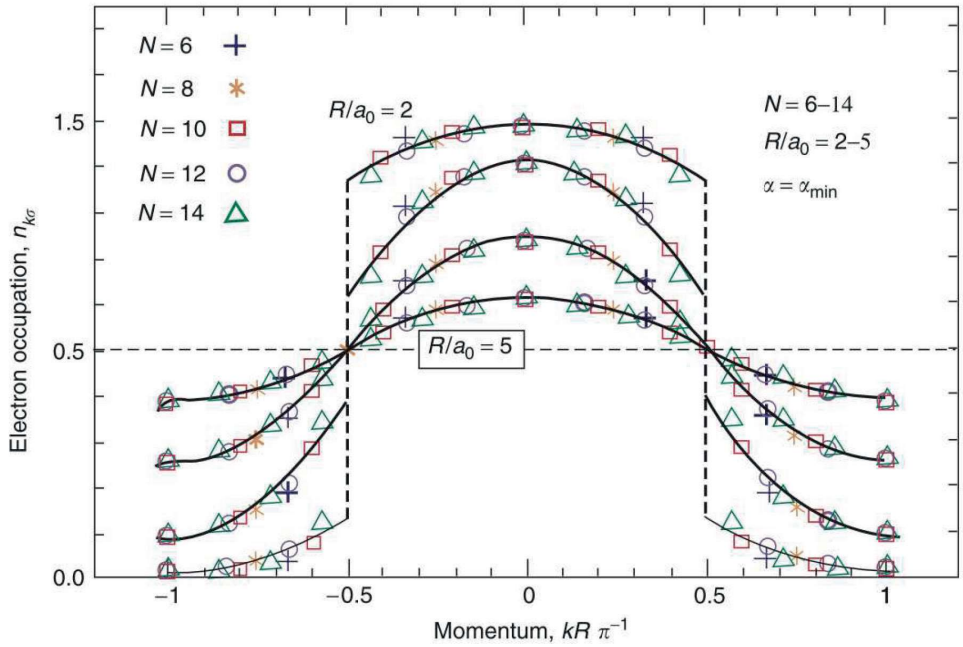

Figure 8.9. Statistical distribution $n_{k\sigma}$ for electrons in a chain of $N = 6$–14 atoms with periodic boundary conditions. The interatomic distance R is specified in units of Bohr radius a_0. The continuous line represents the parabolic interpolation, which is of the same type for both $k > k_F$ and $k < k_F$.

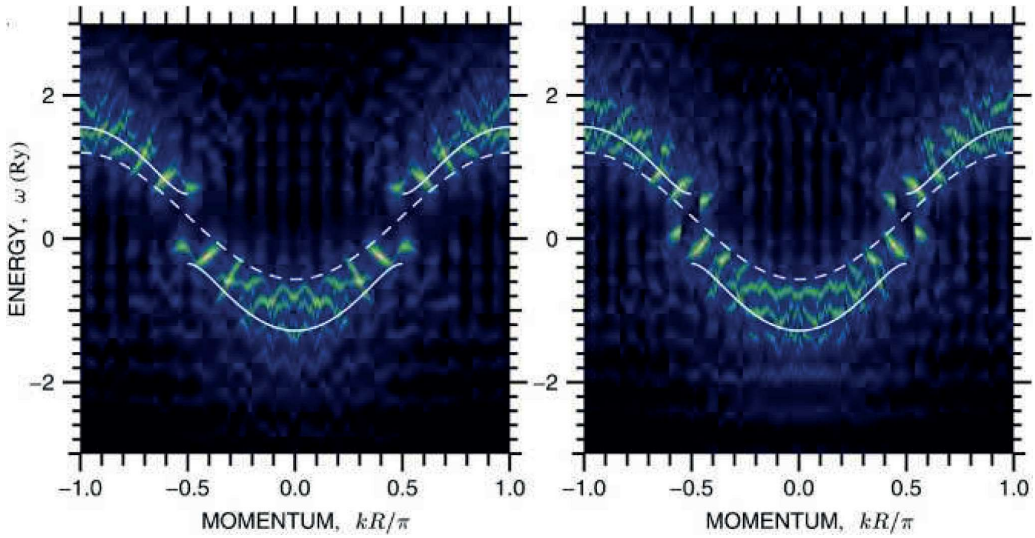

Figure 8.10. Spectral-density-peak positions for the nanochain of $N = 10$ (left panel) and $N = 11$ (right panel) atoms with generalized boundary conditions [8]. The Hartree-Fock (solid line) and noninteracting system (dashed line) dispersion relations are shown for comparison. For an explanation of the splitting located i the middle of the band see main text (for details see Ref. [8]).

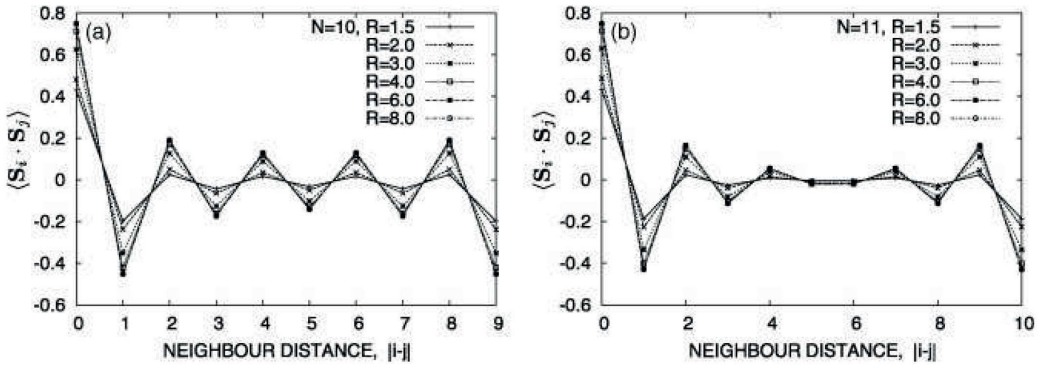

Figure 8.11. Parity effect on spin ordering: spin-spin correlations for nanochains of $N = 10$ (a) and $N = 11$ (b) atoms. The values of the interatomic distance R are specified in the atomic units ($a_0 = 0.529$ Å). The correlations encompases the whole system and thus mimic the long-range ordering of the spin-density wave type (for details see Ref. [8]).

the vertical dashed lines mark the position of Fermi level for this half-filled configuration. Third, the distribution function loses its discontinuous points located $k_F R/\pi = \pm 0.5$ at a critical interacting distance $R \simeq 5a_o$. The smeared out distribution function for $R = 5a_0$ around the value $n_{k\sigma} = 1/2$ defines roughly the transition from the delocalized states of electrons in this nanoscopic system to the localized states, since for $R > 5a_0$ $\boldsymbol{k}$ is not a good quantum number anymore.

Two other characteristics of those correlated nanosystems should be noted. First, we have plotted in Fig. 8.10 the electronic band structure for $N = 10$ and 11 for selected $R \leqslant a_0$.

We observe well defined electronic bands, as marked by the continuous lines. The dashed lines represent the band obtained in the tight binding approximation, when no correlations are included. One feature is striking: the band structure exhibits a well defined gap located at the Fermi wave vector. This may look surprising at first, since no long-range (antiferromagnetic) ordering can be expected for such a small system. However, the picture clarifies when one plots the spin-spin correlation function for those two situations, as shown in Fig. 8.11(a), (b). Note, that the correlation functions encompass the whole length of the chain as if the systems were ordered in an antiferromagnetic manner. In other words, the correlation length is at least of the order of the system size. Thus effectively, the electronic structure has an appearance of a magnetically ordered state, with diminishing magnitude in a quasiperiodic manner, reminiscent of the spin-density-wave state. This is a truly nanoscopic physics, in which both the Slater and the Mott-Hubbard features are present.

In other words, an evolution from atomic physics to the condensed-matter state with itinerant carriers in the latter state is a universal feature, inde-

pendent of the system size. This is more involved when the atomic disorder, in addition to the correlation effects, appears [9].

8.3. Concluding Remarks

In this article we have outlined basic features of systems with metal-insulator transition of the Mott-Hubbard type. These systems are at the forefront of research as they represent on one hand the borderline between the physics of metals and ordering magnets from one side and that of Mott insulators, magnetic semiconductors, and high-temperature superconductors from the other. The theory of strongly correlated system is still in the process of making; available are models and sophisticated band-structure-calculation methods such as DFT-DMFT, LDA+U, etc.

Acknowledgment

The work has bene financially supported through the Grant OPUS No. UMO-2018/29/B/ST3/02646 from Narodowe Centrum Nauki (NCN).

References

[1] E.R. Dobbs: *Helium Three,* Oxford University Press, chapters 3–5.
[2] I. Bloch, J. Dalibard, and W. Zwerger. Rev. Mod. Phys. **80**, 885 (2008).
[3] H. Kuwamoto, J.M. Honig, and J. Appel. Phys. Rev. B **22**, 2626 (1980).
[4] L.D. Landau, Sov. Phys. JETP **3**, 920 (1957); **5**, 101 (1957).
[5] P. Korbel, W. Wójcik, A. Klejnberg, J. Spałek, M. Aquarone, and M. Lavagna, Eur. Phys. J. B **32**, 315 (2003).
[6] J.M. Honig, and J. Spałek, Chem. Mater., **10**, 2910 (1998).
[7] M. Imada, A. Fujimori, and Y. Tokura, Rev. Mod. Phys. **70**, 1039 (1998).
[8] J. Spałek, E.M. Görlich, A. Rycerz, R. Zahorbeński, J. Phys.: Condens. Matter **19**, 255212 (2007), pp. 1–42.
[9] K. Byczuk , W. Hofstetter , and D. Vollhardt , Int. J. Mod. Phys. B **24**, pp. 1727–55 (2010).
[10] J. Spałek, A. Datta, and J. M. Honig, Phys. Rev. B **33**, 4891 (1986); J. Spałek, J. Sol. St. Chem. **88**, pp. 70–93 (1990);
[11] J. Spałek, A Datta, and J.M. Honig, Phys. Rev. Lett. **59**, 728 (1987); J. Spałek, M. Kokowski, and J.M. Honig, Phys. Rev. B **39**, 4175 (1989).

For further reading on the subject see:

[12] J. Spałek in *Reference Module in Materials Science and Materials Engineering* (Elsevier, Oxford, 2016), pp. 1–20.
[13] F. Gebhard, *The Mott Metal-Insulator Transition*, Springer Tracts in Modern Physics, Vol. 137 (1997).
[14] J. Spałek, *Introduction to condensed matter physics* (in Polish: PWN SA, Warszawa 2016; English version to be published by Springer Verlag).